NUMERICAL IMPLEMENTATION AND CALIBRATION OF A HYSTERETIC MODEL WITH PINCHING FOR THE CYCLIC RESPONSE OF STEEL AND COMPOSITE JOINTS

Pedro Nogueiro[1], Luís Simões da Silva[2], Rita Bento[3] and Rui Simões[4]

[1]Department of Applied Mechanics, Polytechnic Institute of Bragança
Bragança, Portugal (nogueiro@ipb.pt)
[2]Department of Civil Engineering, University of Coimbra – Polo II
Pinhal de Marrocos, 3030 Coimbra, Portugal (luisss@dec.uc.pt)
[3]Department of Civil Engineering, Instituto Superior Técnico
Av. Rovisco Pais, Lisboa, Portugal (rbento@civil.ist.utl.pt)
[4]Department of Civil Engineering, University of Coimbra – Polo II
Pinhal de Marrocos, 3030 Coimbra, Portugal (rads@dec.uc.pt)

ABSTRACT

In this paper, a hysteretic model with pinching is presented that is able to reproduce the cyclic response of steel and composite joints. Secondly, the computer implementation and adaptation of the model in a spring element within the computer code Seismosoft is described. The model is subsequently calibrated using a series of experimental test results for steel and composite joints subjected to cyclic loading. Finally, typical parameters for the various joint configurations are proposed.

KEYWORDS

Structural Engineering, Steel Structures, Buildings, Component Method, Beam-to-column Joints, Dynamic Behaviour, Seismic Behaviour, Joint model.

INTRODUCTION

The behaviour of steel or composite joints under cyclic loading is characterized by hysteretic loops with progressive degradation of strength and stiffness that eventually leads to failure of the joint. A typical natural event that, for simplicity, is usually approximated by cyclic loading is an earthquake. Usually, seismic events provoke relatively high amplitudes of rotation in the joint area, so that steel repeatedly reaches the plastic range and the joint fails after a relatively small number of cycles. This typical behaviour is usually called oligocyclic fatigue, in close analogy with the behaviour of steel under repeated cyclic loading stressed into the plastic regime. Because of the inherent complexity of steel and composite joints, characterized by material non-linearity (plasticity, strain-hardening), non-linear contact and slip, geometrical non-linearity (local instability), residual stress conditions and complicated geometrical configurations, the definition of each individual cycle is not easy. In contrast

to the typical static monotonic response of a steel or composite joint, it must be able to reproduce the pinching effect.

Previous work by the authors (Nogueiro *et al.* 2003) investigated the effect of pinching on the seismic response of steel frames and concluded that it results in a variation of about 20% of the joint rotation, thus increasing the ductility demand on the joints to avoid failure. It is the objective of this paper: (i) to present a hysteretic model with pinching based on the Richard-Abbott mathematical model (Richard & Abbott 1975) and developed by Della Corte et al (2000); (ii) to describe the computer implementation and adaptation of the model in a spring element within the computer code SeismoStruct (Seismosoft 2004); (iii) to apply and calibrate the model with a series of experimental test results for steel and composite joints subjected to cyclic loading; and (iv) to compare and propose typical parameters for the chosen joint configurations.

MODIFIED RICHARD-ABBOTT MODEL

The Richard-Abbott model is based on a formula developed in 1975 (Richard & Abbott 1975) to reproduce the elastic-plastic behaviour of several materials and was initially used to simulate the static monotonic response of joints and later applied to cyclic situations (De Martino *et al.*1984), a thorough description being shown in Simões *et al.* (2001). This model was modified by Della Corte *et al.* (2000); to include pinching. To describe pinching, two limit curves are introduced, that represent a lower and an upper bounds to possible M-ϕ values. Both curves have a Richard-Abbott type law, shown in Figure 1a, and are characterised by parameters K_{op}, M_{op}, K_{hp}, n_p (lower bound curve) and K_o, M_o, K_h, n (upper bound curve). Additionally, any generic point (M,ϕ) of the real path is also considered to belong to a Richard-Abbott type curve, where the relevant parameters are defined as follows:

$$K_{ot} = K_{op} + (K_o - K_{op}) \times t \quad (1a)$$

$$M_{ot} = M_{op} + (M_o - M_{op}) \times t \quad (1b)$$

$$K_{ht} = K_{hp} + (K_h - K_{hp}) \times t \quad (1c)$$

$$n_t = n_p + (n - n_p) \times t \quad (1d)$$

The parameter t, ranging in the interval [0,1], defines the transition law from the lower bound to the upper bound curve. It must reproduce, as closely as possible, the shape of the experimental curves and is given by:

$$t = \left[\frac{(\phi / \phi_{\lim})^{t_1}}{(\phi / \phi_{\lim})^{t_1} + 1} \right]^{t_2} \quad (2)$$

where t_1, t_2 and ϕ_{lim} are three experimentally calibrated parameters. Figure 1b illustrates, qualitatively, the resulting pinching behaviour with reference to one single excursion from the origin.

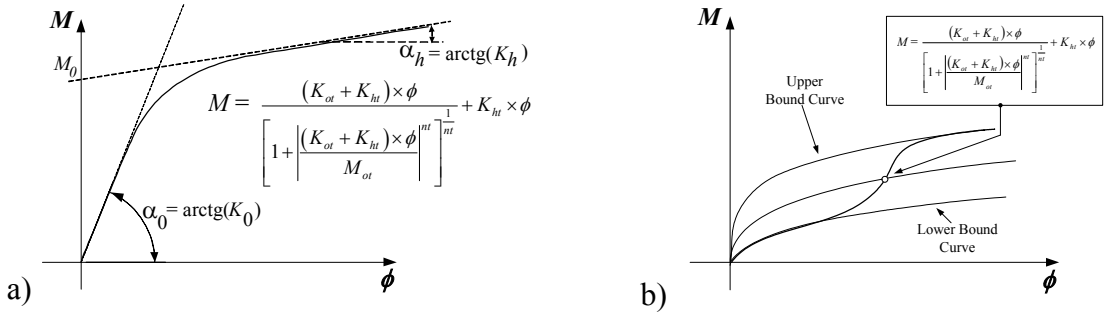

Figure 1: The loading branch without pinching (a) and with pinching (b).

In case of a generic deformation history, the parameter ϕ_{lim} is related to the maximum experienced deformation in the direction of the loading branch to be described. It is evaluated according to the following relationship:

$$\phi_{\lim} = C\left(\left|\phi_o\right| + \phi_{\max}\right) \tag{3}$$

where $\left|\phi_o\right|$ is the absolute value of the deformation corresponding to the starting point of the current excursion, $\phi_{\max}$ is the maximum absolute value of the deformation experienced in the previous loading history, in the direction of loading branch to be described (Figure 2a) and C is a calibration parameter. The unloading branch is assumed to be linear with a slope equal to the initial stiffness K_o up to the interception with the straight line obtained drawing a parallel to the hardening line going through the origin. This allows the Bauschinger effect to be considered.

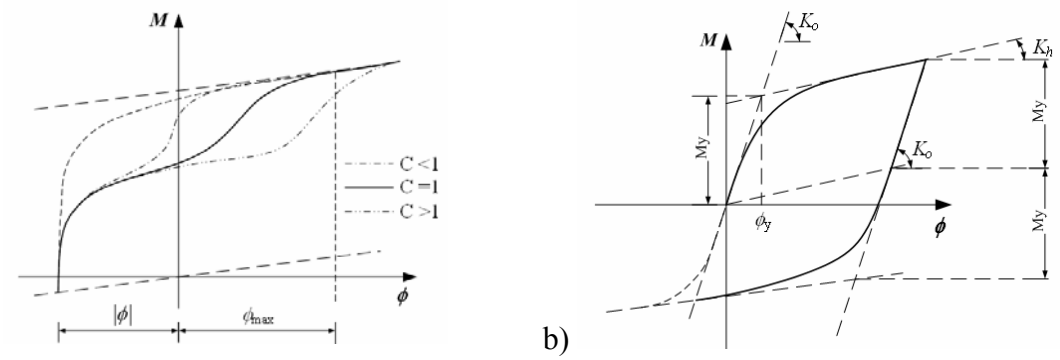

Figure 2: Effect of parameter C (a) and definition of the unloading branch (b).

Cyclic action in the inelastic range produces accumulation of plastic deformation, until ductility of the system is locally exhausted and failure occurs due to fracture. In some cases, the repetition of loading is accompanied by degradation of the structural response because of deterioration of its mechanical properties. This can be taken into consideration both for strength ($M_{o,red}$) and stiffness ($K_{o,red}$) using the following expressions:

$$M_{o,red} = M_o\left(1 - i_M \times \frac{E_h}{M_y \times \bar{\phi}_{u,o}}\right) \qquad K_{o,red} = K_o\left(1 - i_K \times \frac{E_h}{K_o \times \bar{\phi}_{u,o}}\right). \tag{4}$$

$\bar{\phi}_{u,o}$ is the corresponding ultimate value in the case of one single excursion from the origin (monotonic loading), E_h is the hysteretic energy accumulated in all previous experienced excursions, M_y represents the conventional yield resistance of the joint, K_o the initial stiffness as defined in the Figure 2b and coefficient i is an empirical parameter related to damage rate.

Hardening due to cyclic plastic deformation is considered to be isotropic. Besides, experimental results of constant deformation amplitude tests for joints not exhibiting strength deterioration show that cyclic hardening grows up in few cycles and then becomes stable. Therefore, the following assumption is made:

$$\begin{aligned} M_{o,inc} &= M_o && \text{if } \phi_{max} \le \phi_y \\ M_{o,inc} &= M_o\left(1 + H_h \times \frac{\phi_{\max} - \phi_y}{\phi_y}\right) && \text{if } \phi_{max} \ge \phi_y \end{aligned} \tag{5}$$

M_o and $M_{o,inc}$ are the initial and increased value of strength, respectively; ϕ_{max} is the maximum value of deformation reached in the loading history (in either positive or negative direction); ϕ_y is the

conventional yielding value of deformation (see Figure 2); H_h is an empirical coefficient defining the level of the isotropic hardening (Filippou *et al.* 1983). The above formulation practically corresponds to translate the asymptotic line of the original Richard-Abbott (De Martino *et al.*1984), equation as a function of the extent of the plastic deformation.

COMPUTATIONAL IMPLEMENTATION

The numerical implementation of the hysteretic model described above was carried out using the Delphi (Delphi 7, 2002) development platform. A six degree-of-freedom spring element was implemented in the structural analysis software SeismoStruct from Seismosoft (2004). The implementation comprised two major parts. The first consists of the management of the hysteretic cycles, where a clear distinction between positive and negative moment must be made because of possible asymmetry of joint response under hogging or sagging bending. An illustrative flowchart of the cycle management is shown in Figure 3.

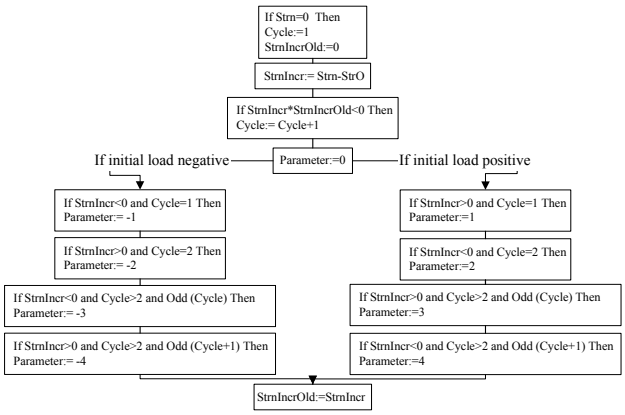

Figure 3: Flowchart for the management of hysteretic cycles.

The second part of the implementation relates to the development of the code for each cycle. Several possibilities must be considered, depending on the starting bending moment (positive or negative) and the sign of the strain increment (positive or negative). In total, 30 parameters have to be defined for this model, fifteen for the ascending branches (subscript *a*) and fifteen for the descending branches (subscript *d*): K_a (and K_d) is the initial stiffness, M_a (and M_d) is the strength, K_{pa} (and K_{pd}) is the post limit stiffness, n_a (and n_d) is the shape parameter, all these for the upper bound curve (see figure 1), K_{ap} (and K_{dp}) is the initial stiffness, M_{ap} (and M_{dp}) is the strength, K_{pap} (and K_{pdp}) is the post limit stiffness, n_{ap} (and n_{dp}) is the shape parameter, all these for the lower bound curve, t_{1a} and t_{2a} (and t_{1d} and t_{2d}) are the two parameters related to the pinching, C_a (and C_d) is the calibration parameter related to the pinching, normally equal to 1 (see figure 2), i_{Ka} (and i_{Kd}) is the calibration coefficient related to the stiffness damage rate, i_{Ma} (and i_{Md}) is the calibration coefficient related to the strength damage rate, H_a (and H_d) is the calibration coefficient that defines the level of isotropic hardening and E_{maxa} (and E_{maxd}) is the maximum value of deformation.

To illustrate the application and versatility of the model, it was tested on a typical steel joint with its properties defined in Table 1, with stiffness and strength deterioration but no hardening.

TABLE 1
JOINT PARAMETERS

K_a KNm/rad	M_a KNm	K_{pa} KNm/rad	n_a	K_{ap} KNm/rad	M_{ap} KNm	K_{pap} KNm/rad	n_{ap}	t_{1a}	t_{2a}	C_a	i_{Ka}	i_{Ma}	H_a	E_{maxa} rad
34440	116	1700	2	34440	60	1700	1	10	0.15	1	15	0.01	0	0.1
K_d KNm/rad	M_d KNm	K_{pd} KNm/rad	n_d	K_{dp} KNm/rad	M_{dp} KNm	K_{pdp} KNm/rad	n_{dp}	t_{1d}	t_{2d}	C_d	i_{Kd}	i_{Md}	H_d	E_{maxd} rad
44440	136	1700	2	44440	80	1700	1	10	0.15	1	15	0.01	0	0.1

Firstly two monotonic loadings were considered, one positive and another negative. Subsequently, two distinct cyclic load histories were applied (ECCS load history and an random load history). The results, illustrated in Figure 4, show that, for low rotations ($< \theta_y$), the cyclic results coincide with the monotonic results. With increased rotation, the cyclic response deviates from the monotonic response because of strength and stiffness deterioration.

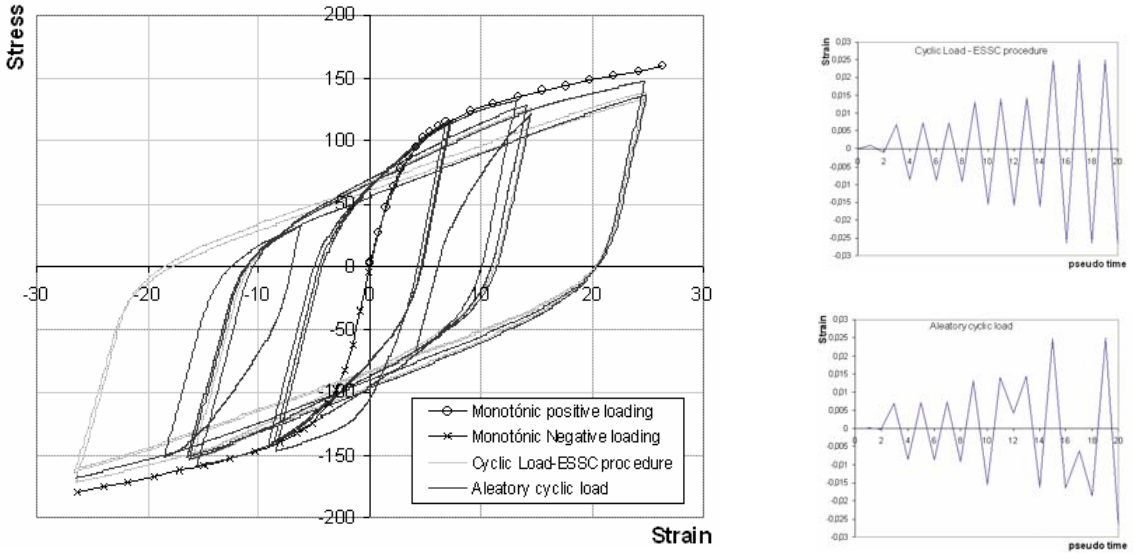

Figure 4: Hysteretic and monotonic curves.

APPLICATION AND VALIDATION

In order to establish reliable parameters for a range of end-plate beam-to-column steel and composite joint configurations and to validate the accuracy of the model, a group of well-documented experimental results were selected from the literature. These tests were performed by Simões *et al.* (2001), Dubina *et al.* (2002) and Liew *et al.* (2004) and are summarized in Table 2.

TABLE 2
EXPERIMENTAL TESTS

Nº	Test Ref.	Author	Type	Beam	Column	h_c cm	M^+_y KNm	M^-_y KNm	K^+_y KNm/rad	K^-_y KNm/rad
1	E9	Simões	External	IPE270	HEA220	12	114	115	24570	26810
2	E10	Simões	External	IPE270	HEA220+C	12	170	159	36950	40830
3	E11	Simões	Internal	IPE270	HEA220	12	83	81	16500	18830
4	E12	Simões	Internal	IPE270	HEA220+C	12	117	118	34440	36220
5	BX-CUC1	Dubina	Internal	Fig.7	Fig.7	12	143	137	36870	37920
6	BX-CUC2	Dubina	Internal	Fig.7	Fig.7	12	143	137	36870	37920
7	CJ2	Liew	Internal	305x305xUB50	305x305x97UC	12	165*	150*	27648	16987
8	CJ4	Liew	Internal	305x305xUB50	305x305x97UC+S	12	190*	165*	42697	45118
9	BX-CSC1**	Dubina	Internal	Fig.7	Fig.7	12	195	150	102500	75050

HEA220+C (concrete); 305x305x97UC+S (Stiffening of column wed). *Estimated value. **Symmetrical test

Ideally, the initial stiffness, moment resistance and post-limit stiffness should be obtained directly from complementary monotonic tests, as was the case for all tests except for tests 7 and 8. The cyclic tests are thus best used to find the strength and stiffness deterioration coefficients, the isotropic hardening, and the pinching parameters.

Tests 1 and 2 are external joints. All other tests correspond to internal joints. Tests 2 and 4 have the column encased in concrete. All tests are loaded anti-symmetrically, except for test 9. Test 8 has the column web stiffened with a doubler plate (Figure 10d). All concrete slabs have 12 cm thickness and

continuous steel reinforcement around the column. Figures 5 to 10 illustrate the joint details and the corresponding experimental and analytical hysteretic curves.

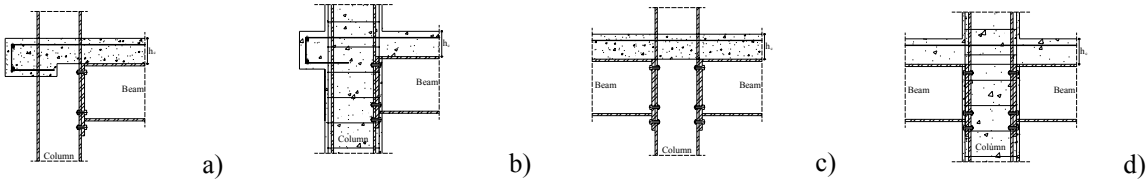

Figure 5: Joints 1 (a), 2 (b), 3 (c) and 4 (d) – Simões et al. [6].

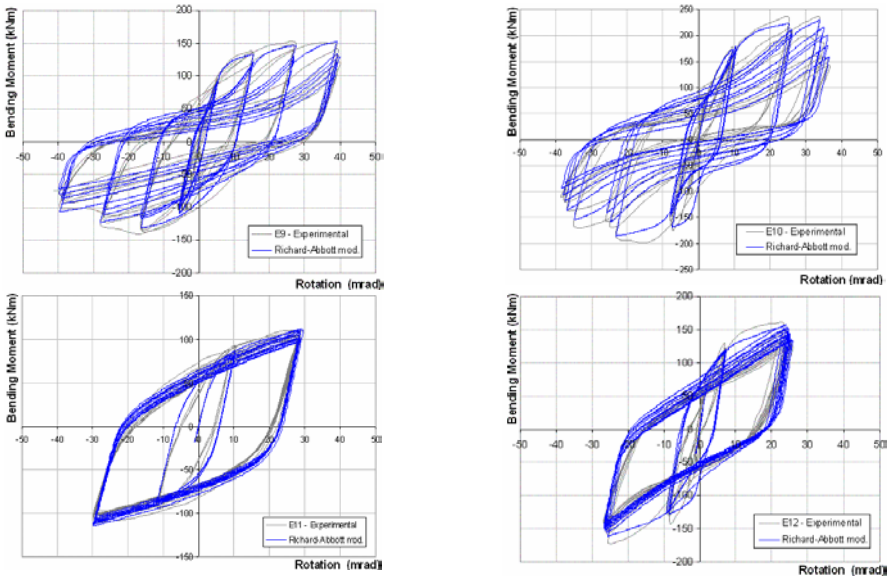

Figure 6: Hysteretic curves for joints 1 to 4.

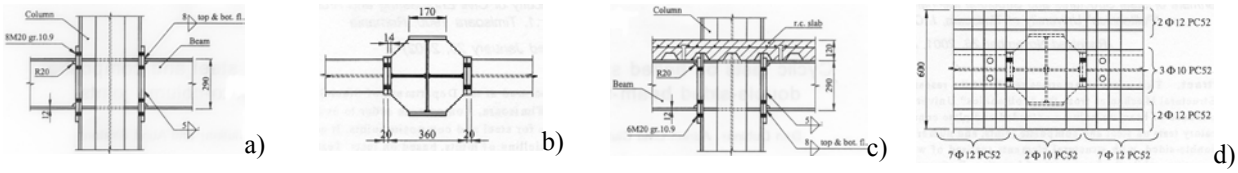

Figure 7: Bare steel joint 5 and 6 (a), (b) and composite joint 9 (c), (d) – Dubina et al. [9].

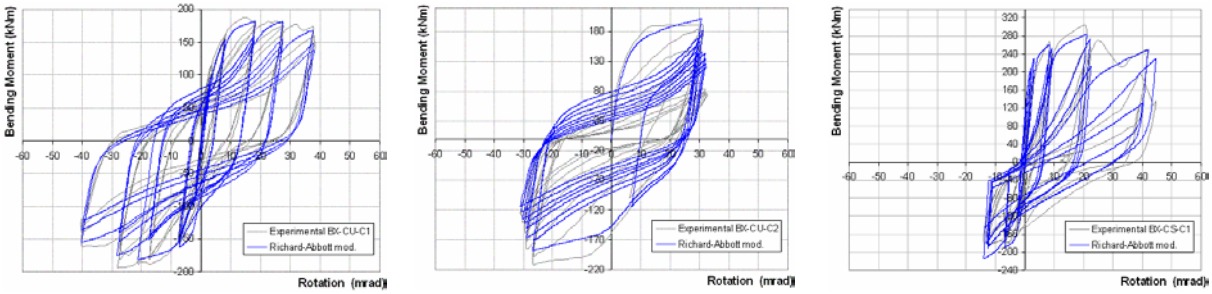

Figure 8: Hysteretic curves for joints 5, 6 and 9.

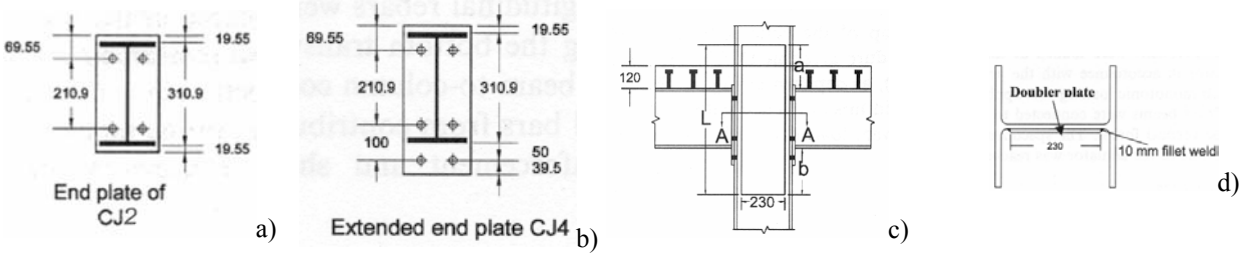

Figure 9: End plate for joints 7 (a) and 8 (b), composite joint 8 (c) and web stiffener (d) – Liew et al. [10].

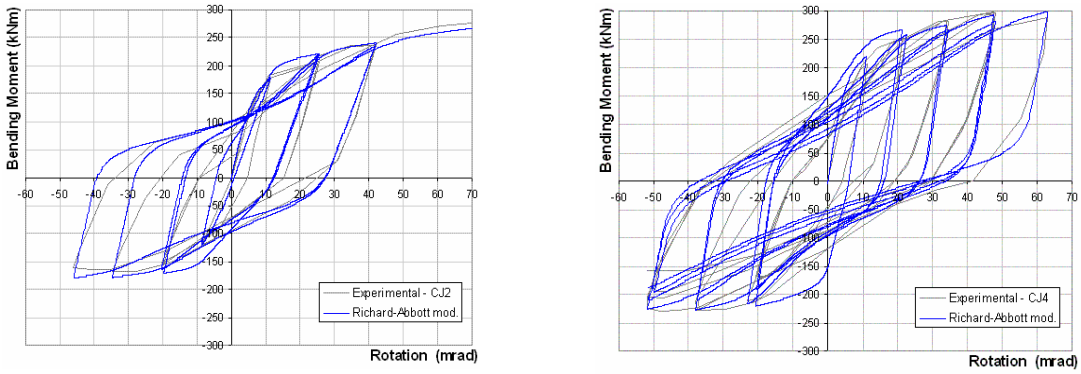

Figure 10: Hysteretic curves for joints 7 and 8.

It is noted that tests 5 and 6, although structurally identical, were subjected to different cyclic loading procedures. Globally, the model is able to accurately reproduce all experimental results. Tables 3 and 4 summarise the results for all parameters for the nine tests.

TABLE 3
JOINT PARAMETERS FOR ALL TESTS FOR THE ASCENDING BRANCHES

Test N°	1	2	3	4	5/6	7	8	9**	Ref. Value
$\mathbf{K_a}$ KNm/rad	24570	36950	16500	34400	36870	27648	42697	102500	$\mathbf{K^+_y}$
$\mathbf{M_a}$ KNm	130	200	85	117	170	200	230	240	$\mathbf{1.2\times M^+_y}$
$\mathbf{K_{pa}}$ KNm/rad	600	1025	825	1700	1100	691	1280	3000	$\mathbf{0.03\times K^+_y}$
$\mathbf{n_a}$	2	2	2	2	2	2	2	2	**2**
$\mathbf{K_{ap}}$ KNm/rad	24570	36950	16500	34400	36870	27648	42697	102500	$\mathbf{K^+_y}$
$\mathbf{M_{ap}}$ KNm	70	120	40	60	100	100	115	1**	**0.65× Ma**
$\mathbf{K_{pap}}$ KNm/rad	600	1025	825	1700	1100	660	1280	3000	$\mathbf{0.03\times K^+_y}$
$\mathbf{n_{ap}}$	1	1	1	1	1	1	1	1	**1**
$\mathbf{t_{1a}}$	15	10	6	10	15	15	15	15	6<...<15
$\mathbf{t_{2a}}$	0.5	0.5	0.15	0.15	0.5	0.2	0.15	0.2	0.15<...<0.5
$\mathbf{C_a}$	1	1	1	1	1	1	1	1	**1**
$\mathbf{i_{Ka}}$	15	20	3	15	25	3	20	25	3<...<25
$\mathbf{i_{Ma}}$	0.04	0.05	0.01	0.01	0.04	0.1	0.01	0.4	0.01<..<0.1
$\mathbf{H_a}$	0.04	0.04	0.04	0.02	0.01	0.04	0.02	0.02	0.01<..<0.04
$\mathbf{E_{maxa}}$ rad	0.1	0.1	0.1	0.1	1	0.01	0.1	0.1	0.1

TABLE 4
JOINT PARAMETERS FOR ALL TESTS FOR THE DESCENDING BRANCHES

Test N°	1	2	3	4	5/6	7	8	9**	Ref. Value
$\mathbf{K_d}$ KNm/rad	26810	40830	18830	36220	37920	16987	45118	75050	$\mathbf{K^-_y}$
$\mathbf{M_d}$ KNm	125	170	80	118	167	180	200	175	$\mathbf{1.2\times M^-_y}$
$\mathbf{K_{pd}}$ KNm/rad	670	1020	940	1800	1140	425	1250	3250	$\mathbf{0.03\times K^+_y}$
$\mathbf{n_d}$	2	2	2	2	2	2	2	2	**2**
$\mathbf{K_{dp}}$ KNm/rad	26810	40830	18830	36220	37920	16987	45118	75050	$\mathbf{K^-_y}$
$\mathbf{M_{dp}}$ KNm	60	75	60	60	110	90	100	110	**0.65× Md**
$\mathbf{K_{pdp}}$ KNm/rad	670	1020	940	1800	1140	425	1250	3250	$\mathbf{0.03\times K^+_y}$
$\mathbf{n_{dp}}$	1	1	1	1	1	1	1	1	**1**
$\mathbf{t_{1d}}$	6	15	5	20	20	20	20	20	5<...<20
$\mathbf{t_{2d}}$	0.2	0.5	0.15	0.15	0.2	0.15	0.15	0.5	0.15<...<0.5
$\mathbf{C_d}$	1	1	1	1	1	1	1	1	**1**
$\mathbf{i_{Kd}}$	18	20	1	5	15	1	10	15	1<...<20
$\mathbf{i_{Md}}$	0.06	0.08	0.01	0.01	0.06	0.01	0.01	0.01	0.01<..<0.08
$\mathbf{H_d}$	0	0	0.02	0	0	0	0	0	0
$\mathbf{E_{maxd}}$ rad	0.1	0.1	0.1	0.1	0.1	0.1	0.1	0.1	0.1

Examination of the variation of the non-dimensional properties for the nine tests reveals that, except for tests 3 and 4, that present some deviations from the remaining tests (because they were only subjected to moderate rotations and did not reach collapse), the structural properties for strength and stiffness were fairly constant. These values can be seen in the last column of Tables 3 and 4. For the calibration parameters, it was not possible to find a clear tendency. This results from the small number of tests that are used and the variation of joint characteristics. Thus, for these parameters, a range of values is presented that covers all tested joints.

CONCLUSIONS

This paper presents the numerical implementation of a hysteretic model able to simulate a generic cyclic steel-composite joint behaviour. It is incorporated in the structural analysis software SeismoStruct (Seismosoft 2004); as a joint element, thus allowing realistic nonlinear static and dynamic structural analyses. The model was applied to nine experimental joint tests from three independent sources, showing a very good agreement with the experimental results, even when using different cyclic loading strategies. Despite the small sample size, a clear trend was observed for the required model parameters for end-plate beam-to-column composite joints. This may lead to the proposal of design parameters for such joints, an issue that is currently being pursued by the authors with an enlarged sample of test results.

ACKNOWLEDGEMENTS

Financial support from the Portuguese Ministry of Science and Higher Education (*Ministério da Ciência e Ensino Superior*) under contract grants from *PRODEP III (5.3)* for Pedro Nogueiro is gratefully acknowledged. The assistance provided by Seismosoft, is also most appreciated (http://www.seismosoft.com).

REFERENCES

Della Corte, G., De Matteis, G. and Landolfo, R. (2000). Influence of Connection Modelling on Seismic Response of Moment Resisting Steel Frames. In: Mazzolani FM, editor. *Moment resistant connections of steel buildings frames in seismic areas*, E. & F.N. Spon, London.

Delphi 7. (2002). Borland Software Corporation.

De Martino, A., Faella, C. and Mazzolani, F. M. (1984). Simulation of Beam-to-Column Joint Behaviour under Cyclic Loads. *Construzioni Metalliche* **6,** 346-356.

Dubina, D., Ciutina, A.L. and Stratan, A. (2002). Cyclic tests on bolted steel and composite double-sided beam-to-column joints. *Steel and Composite Structure* **Vol. 2, N.º 2,** 147-160.

Filippou F. C., Popov, E. P., Bertero, V. V. (1983). Effect of Bond deterioration on Hysteretic behaviour of reinforced concrete joints. *Report Nº UCB/EERC-83/19*, Earthquake Engineering Research Center, University of California, Berkeley.

Liew, J.Y.R., Teo, T.H. and Shanmugam, N.E. (2004). Composite joints subject to reversal of loading – Part 1: experimental study. *Journal of Constructional Steel Research* **60,** 221-246.

Nogueiro, P., Simões da Silva, L. and Bento, R. (2003). Influence of joint slippage on the cyclic response of steel frames, paper 66, in Topping, B.H.V. (ed.), *Proceedings of 9th International Conference on Civil and Structural Engineering Computing*, Civil-Comp Press, Stirling, United Kingdom.

Richard, R. M. and Abbott, B. J. (1975). Versatile Elasto-Plastic Stress-Strain Formula. *Journal of the Engineering Mechanics Division*, ASCE **101, EM4,** 511-515.

SeismoStruct. (2004). "Computer program for static and dynamic nonlinear analysis of framed structures" [online]. Available from URL: http://www.seismosoft.com

Simões, R., Simões da Silva, L. and Cruz, P. (2001). Behaviour of end-plate beam-to-column composite joints under cyclic loading. *International Journal of Steel and Composite Structures* **1(3),** 355-376.